Transition from Disorder to Order in Thin Metallic Films Studied with Angle-Resolved Photoelectron Spectroscopy

Dah-An Luh,[1,2,*] Cheng-Maw Cheng,[2] Chi-Ting Tsai,[1] Ku-Ding Tsuei,[2,3] and Jian-Ming Tang[4]
[1]*Department of Physics, National Central University, Taoyuan 32001, Taiwan*
[2]*National Synchrotron Radiation Research Center, Hsinchu 30076, Taiwan*
[3]*Department of Physics, National Tsing Hua University, Hsinchu 30013, Taiwan*
[4]*Department of Physics, University of New Hampshire, Durham, New Hampshire 03824, USA*
(Received 14 October 2007; published 16 January 2008)

The transition from disorder to order in Ag film grown on Au(111) was investigated by monitoring the quantum well states using angle-resolved photoelectron spectroscopy. Our results show that the binding energies do not alter, but the in-plane dispersion alters from flat to parabolic when the film is annealed. We suggest that there are isolated and ordered patches scattered across the film at an early stage of the transition and that atoms inside the patches are fully ordered along the surface normal. These ordered patches grow and merge together as the annealing temperature increases.

DOI: 10.1103/PhysRevLett.100.027603 PACS numbers: 79.60.−i, 64.60.Cn, 68.55.A−, 73.21.−b

Construction of thin metallic films on metal or semiconductor substrates continues to attract great interest for both technological and scientific reasons. Atomically flat films are particularly important because they provide not only a well defined foundation on which to construct nanodevices but also a platform with which to manipulate physical properties through the quantum size effect. Much effort has been devoted to finding recipes to grow layer by layer, but in many heteroepitaxial systems that mode of growth does not exist. To address this issue, a two-step growth method for flat and thin metallic films was proposed and is gaining popularity. A film can be grown in a quasi-layer-by-layer mode on depositing materials at a low temperature [1–3]. Because surface atoms are poorly mobile at a low temperature, the film comprises randomly deposited nanoclusters [2,3] and exhibits disorder according to measurement of its electronic band structure [1]. Such a disordered film can transform into a highly ordered and atomically flat film through annealing at an appropriate temperature. With this growth method, many flat and thin metallic films have been grown and investigated, including Ag/GaAs(110) [1,2], Ag/Si [3–5], Ag/Fe(100) [6], Mg/Si(111) [7], and Pb/Si(111) [8,9] among others. In many of these experiments, electronic states in flat and thin metallic films are found to be quantized, and appear as quantum well states (QWS) in photoemission spectra [1,3–8]. Measurements of the in-plane dispersion of QWS reveal also the nature of thin metallic films that can be two-dimensional [4], quasi-one-dimensional [5], or zero dimensional [1].

Although the two-step method of growth has thus yielded many beautiful results, how a disordered film transforms into an ordered film remains a question that is seldom asked but important for our understanding of the structural and electronic properties of thin films and other nanostructures. In this Letter, using Ag/Au(111) as a test system, we demonstrate that the transition from disorder to order in a thin metallic film becomes explored on monitoring the dispersion of its quantized states. In our experiments, thin Ag films are grown on Au(111) by the two-step method and the in-plane dispersion of quantized states in the Ag film is measured in real time using angle-resolved photoelectron spectroscopy (ARPES). Our results show that these quantized states have flat in-plane dispersion in a partially ordered Ag film, and nearly free-electron-like in-plane dispersion in a well ordered Ag film. A model of film crystallization is proposed to explain qualitatively the variation of the in-plane dispersion during annealing.

The ultra-high-vacuum system in which experiments were performed consists of a preparation chamber and a photoemission analysis chamber; the base pressure was better than 1×10^{-10} torr. A Au(111) substrate was mounted on a constructed manipulator, of which the temperature is variable from 37 to 1000 K. The sample temperature was determined with a thermocouple junction (type E) mounted right beside the Au(111) substrate. A clean Au(111) surface was prepared through numerous cycles of Ar ion sputtering and annealing at ~500 °C until photoemission spectra exhibited a sharp and split Au(111) surface state [10,11]. Highly pure Ag was evaporated from a Mo crucible heated by e-beam bombardment onto Au(111) at 37 K. The deposition rate was ~0.3 monolayer (ML) per minute determined with a quartz crystal microbalance; 1 ML denotes one layer of Ag on Ag(111), $\sim 1.39 \times 10^{15}$ atoms/cm^2. The vacuum system was installed on Beamline 21B1 in the National Synchrotron Radiation Research Center at Hsinchu, Taiwan. Photoemission spectra were recorded with an electron energy analyzer (SCIENTA SES 200) equipped with a two-dimensional channel plate and a charge-coupled-device camera, which allows 52 spectra at various emission angles to be collected simultaneously with an angular resolution 0.25°. Our measurements of the in-plane dispersion probed the k space ~ 0.2 Å^{-1} about the $\bar{\Gamma}$ point, which is sufficient to cover the projected band edge of bulk Au. Because both Ag and Au band structures about the $\bar{\Gamma}$ point are nearly identical in all directions, the results from the measurements of only the in-plane wave vector, $k_{\|}$, along $\bar{\Gamma}\bar{K}$ are presented in this Letter. To monitor the variation of the in-plane dispersion, we measured photoemission spectra in real time during sample annealing. The annealing temperature was increased slowly to ensure that all temperature-dependent transitions were recorded.

Photoemission measurements were conducted on Ag/Au(111) thin films with varied Ag coverage. Photons of energy 20 eV were used in all photoemission measurements. Figure 1 displays typical photoemission data showing the variation in the electronic states when a Ag/Au(111) thin film is grown with the two-step method. Figures 1(a), 1(c), and 1(e) show the photoemission intensity plotted against the binding energy and $k_{\|}$; the binding energy has been shifted to have a zero binding energy at the Fermi edge. The in-plane dispersion, $E(k)$, of the electronic states in the thin film is readily identified in these two-dimensional intensity plots. The energy distribution curves of normal emission in Figs. 1(a), 1(c), and 1(e) are plotted in Figs. 1(b), 1(d), and 1(f), respectively. Figures 1(a) and 1(b) are photoemission data from a clean Au(111) surface at 37 K; a sharp and split surface state with a binding energy 0.47 eV agrees with previous work and indicates a good quality of the Au(111) surface [10,11]. Figures 1(c) and 1(d) display photoemission data measured after Ag (22 ML) was deposited on a clean Au(111) surface at 37 K. The data show a flat and featureless background with the Fermi edge, which indicates the disordered nature of the Ag film; this property is expected because Ag atoms have slight mobility on Au(111) at low temperature. During growth, Ag atoms are deposited randomly onto Au(111) to form an amorphous film or a film comprising randomly deposited small clusters [1–3]. Growth of this type is considered to be a quasi-layer-by-layer mode, which yields a flat film with no macroscopic structure [1]. Figures 1(e) and 1(f) show photoemission data from an Ag film (22 ML) on Au(111) annealed and measured at 258 K. A sharp and intense feature appears near the Fermi edge, and three parabolic bands with greater binding energies are clearly observable: these are the Ag surface state and QWS in the Ag film [12]. The sharp Ag surface state demonstrates unequivocally that the Ag film is crystallized and that the surface is Ag(111). The three QWS have binding energies 0.47, 0.73 and 1.01 eV at normal emission, consistent with previous results [12]. The parabolic dispersion indicates that the QWS are nearly free-electron-like in the in-plane direction [4,13]. The dashed line in Fig. 1(e) is the projected band edge of the Au bulk. The QWS evidently do not extend beyond the Au band gap because this gap provides a proper confinement for the QWS to exist.

To explore how the in-plane dispersion evolves from being featureless to nearly free-electron-like, we monitored the in-plane dispersion during sample annealing. For a cursory glimpse at the variation of the electronic states during annealing, Fig. 2 shows a stacking plot of the energy distribution curves of normal emission from Ag (22 ML) on Au(111) annealed at the indicated temperatures. The spectra evidently vary as the annealing temperature increases. At a temperature less than 165 K, the spectra display the Fermi edge without other noticeable features. From 165 to 176 K, a surface state and QWS begin to appear. The weak and broad states indicate that a small part of the Ag film becomes ordered. The surface state and the QWS become clear in the spectrum at 180 K. The great variation of the spectra indicates that a transition from disorder to order in the film structure dependent on temperature occurs between 176 and 180 K. At a tempera-

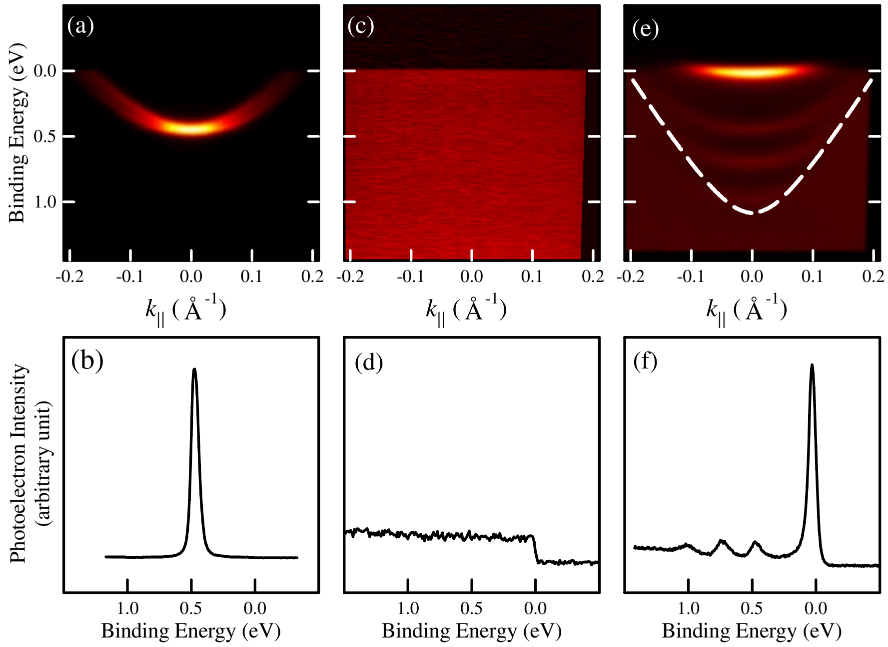

FIG. 1 (color online). Photoemission data showing the variation of electronic states in a Ag/Au(111) thin film during two-step growth. All spectra are measured with photons of energy 20 eV. (a),(c), and (e) present the photoemission intensity plotted against binding energy and $k_{\|}$, and their energy distribution curves of normal emission appear in (b),(d), and (f), respectively. (a) and (b) are measured from clean Au(111) at 37 K. (c) and (d) are measured after Ag (22 ML) is deposited on Au(111) at 37 K. (e) and (f) are measured from Ag (22 ML) on Au(111) annealed at 258 K. The dashed line in (e) is the projected band edge of bulk Au.

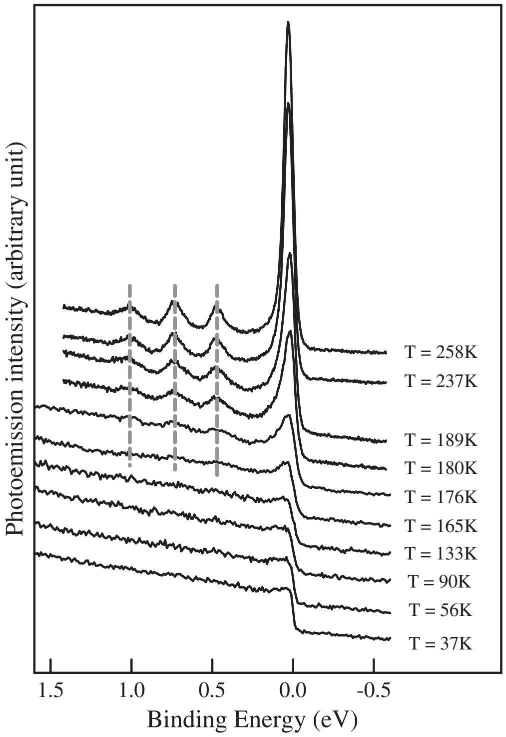

FIG. 2. Energy distribution curves of normal emission from Ag (22 ML) on Au(111) annealed at the indicated temperatures; intensities have been scaled variously for stacking presentation.

ture greater than 180 K, these normal-emission spectra vary little except that the surface state and the QWS continue to enlarge, and become fully developed at 258 K.

Beyond the determination of the transition temperature, an interesting feature observable in Fig. 2 is that the binding energies of QWS remain constant as they appear at 176 K, as indicated with dashed lines. According to the phase accumulation model [12], the binding energies of QWS are determined by the band structure, the film thickness, and the phase shifts at the film surface and the interface between the film and the substrate. The fact that the binding energies of QWS remain constant indicates that all parameters in the phase accumulation model remain roughly the same during film crystallization. Even at an initial stage of film crystallization when only a small part of the film has become ordered, the thickness of the ordered part of the film and its interface between the film and the substrate are similar to, if not the same as, those in a fully ordered film.

Further features are observable on comparison of the in-plane dispersions of QWS at various stages of annealing. Figure 3 shows three two-dimensional maps of photoemission intensity measured at various temperatures. The variation of the in-plane dispersion during annealing is remarkable. When the sample is annealed at 180 K, the QWS have flat in-plane dispersion, as shown in Fig. 3(a); such flat in-plane dispersion has been observed when the sample is annealed at 176 K (not presented here) but it is weak and broad. When the sample is annealed at 258 K, the QWS have parabolic dispersion, as shown in Fig. 3(c). Figure 3(b) is somewhat complicated: the dispersion spreads as $|k_{\parallel}|$ increases, likely as an overlap of flat and parabolic dispersions. To determine the in-plane effective masses of the QWS, $m^*_{\parallel}$, in Fig. 3(c), we fitted second-order polynomials to the dispersion; the results are drawn as dashed lines in the figure. Values of $m^*_{\parallel}/m_e$ from the fitting are 0.36, 0.35, and 0.39 for the three QWS with binding energies 0.47, 0.73, and 1.01 eV, respectively; m_e is the free electron mass. The fit is very good and these numbers conform to those reported for similar systems [4,5,13]. For a similar analysis applied on Fig. 3(a), the flat dispersions yield large effective masses ($> 3m_e$), as expected. The fitted results from both Figs. 3(a) and 3(c) are plotted in Fig. 3(b); their satisfactory match with the dispersion strengthens the idea that the dispersion in Fig. 3(b) is an overlap of flat and parabolic dispersions.

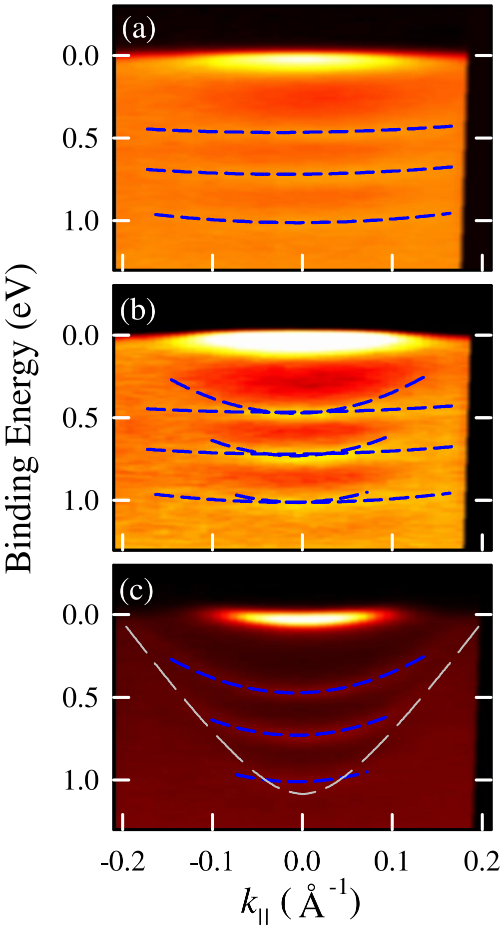

FIG. 3 (color online). Intensity of photoemission plotted against binding energy and $k_{\parallel}$ at various stages of annealing. The annealing temperatures are (a) 180, (b) 189, and (c) 258 K. The short blue dashed lines are the fitting results of the QWS peak positions. The long white dashed line in (c) is the projected band edge of bulk Au.

The in-plane dispersions are related closely to the characteristic length scale of the electron wave functions along

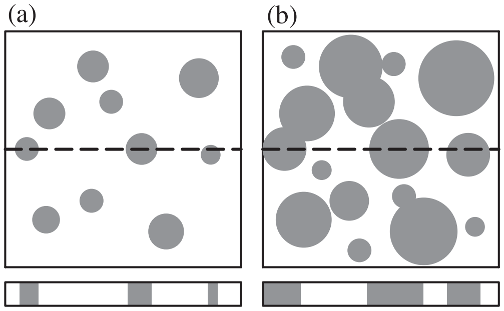

FIG. 4. Sketches to illustrate a metallic thin film at (a) initial and (b) middle stages of the transition from disorder to order. The upper figures are the view on the film along the surface normal; the lower figures are the view along the in-plane direction cutting through the film at the place indicated by the dashed line. A gray area indicates an ordered region, whereas a white area indicates a disordered region.

the in-plane directions. In Fig. 3(a), the flat dispersion is an indication that the QWS lack translational symmetry in the in-plane direction; these states are thus localized, as expected, because only a small part of the film shows order when the sample is annealed at 180 K. The parabolic dispersion in Fig. 3(c) implies that QWS are nearly free-electron-like, as likewise expected because the entire film is well ordered at 258 K: translational symmetry exists in the in-plane direction. The overlapped dispersion in Fig. 3(b) shows that small and isolated ordered domains coexist with larger ordered domains in the film during the transition from disorder to order.

A summary of discussion on Figs. 2 and 3 provides a clear picture how a disordered Ag film transforms into a well ordered film through annealing, as illustrated by the sketches in Fig. 4. When Ag is deposited on Au(111) at a low temperature, the film grows in a quasi-layer-by-layer mode. Although the film is disordered, its thickness is similar across the entire film. The film initially orders on annealing about the transition temperature. The flat dispersion in Fig. 3(a) indicates that the ordered part of the film comprises small and isolated ordered patches scattered across the film, as illustrated in Fig. 4(a). That binding energies of QWS remain constant during annealing in Fig. 2 indicates that the film is completely ordered throughout, along the surface normal inside these isolated ordered patches, even at an initial stage of the transition. As the annealing temperature increases, the isolated ordered patches expand and likely merge, as shown in Fig. 4(b). Some patches are still small and isolated, but others are large enough to have $k_{\|}$ defined. During the transition from disorder to order, patches of both kinds coexist in the film, as the overlapped dispersion in Fig. 3(b) implies. After annealing is complete, the dispersion is parabolic and has well defined binding energies along the surface normal, as shown in Fig. 3(c). The entire film is thus crystallized and flat with little variation of thickness.

When the isolated ordered patches are large enough to have $k_{\|}$ defined, one might query why the quantization in $k_{\|}$ is not observed in the dispersion. Of two reasons for the missing quantization in $k_{\|}$ in the photoemission data, first, the lateral confinement is poorly defined because of the disordered nature of the boundary of the order patches, and, second, there might be a substantial variation of the size and shape of the ordered patches. Both factors make $k_{\|}$ act as a continuous variable macroscopically in photoemission measurements.

In principle one might determine the characteristic size of ordered patches by analyzing the spacing between the quantized $k_{\|}$. Missing quantization in $k_{\|}$ in our measurements suggests that there is a wide size distribution of ordered patches during transition. It is not trivial for photoemission measurements to determine the size of structures on an inhomogeneous surface. Such a technique with nanoscale spatial resolution as scanning probe microscopy might be more suitable to determine the size of ordered patches during the transition from disorder to order.

The signals used to monitor the transition from disorder to order are not limited to those from QWS: the variation in dispersion during annealing is observed also for the surface state in Fig. 3. One expects the monitoring of electronic states with ARPES in real time to be useful to characterize ordering processes in general, but the effectiveness of the technique depends strongly on the representation of the order in system structures by monitoring signals.

In summary, we have demonstrated that the transition from disorder to order in a thin metallic film can be explored on monitoring the in-plane dispersion of its quantized states during annealing. The thin Ag/Au(111) film grown with the two-step method was studied as a test system, and a detailed picture of how a disordered Ag film becomes crystallized is derived from the results from temperature-dependent ARPES measurements.

National Science Council, Taiwan (Grant No. NSC-95-2112-M-008-012) and National Synchrotron Radiation Research Center, Taiwan, supported this work.

---

*luh.dah.an@gmail.com

[1] D. A. Evans *et al.*, Phys. Rev. Lett. **70**, 3483 (1993).
[2] A. R. Smith *et al.*, Science **273**, 226 (1996).
[3] I. Matsuda *et al.*, Phys. Rev. B **63**, 125325 (2001).
[4] I. Matsuda *et al.*, Phys. Rev. B **65**, 085327 (2002).
[5] N. Nagamura *et al.*, Phys. Rev. Lett. **96**, 256801 (2006).
[6] J. J. Paggel *et al.*, Phys. Rev. Lett. **81**, 5632 (1998).
[7] L. Aballe *et al.*, Phys. Rev. B **65**, 125319 (2002).
[8] M. H. Upton *et al.*, Phys. Rev. Lett. **93**, 026802 (2004).
[9] Y. Guo *et al.*, Science **306**, 1915 (2004).
[10] S. LaShell *et al.*, Phys. Rev. Lett. **77**, 3419 (1996).
[11] F. Reinert *et al.*, Phys. Rev. B **63**, 115415 (2001).
[12] T. Miller *et al.*, Phys. Rev. Lett. **61**, 1404 (1988).
[13] M. A. Mueller *et al.*, Phys. Rev. B **41**, 5214 (1990).